Ex vivo osteochondral test system with control over cartilage defect depth – a pilot study to investigate the effect of oxygen tension and chondrocyte-based treatments in chondral and full thickness defects in an organ model

Andrea Schwab [1], Alexa Buss [1], Oliver Pullig [1, 2], Franziska Ehlicke [1,$]

[1] University Hospital Wuerzburg, Department Tissue Engineering and Regenerative Medicine, Roentgenring 11, 97070 Wuerzburg, Germany

[2] Fraunhofer Institute for Silicate Research ISC, Translational Center Regenerative Therapies, Roentgenring 11, 97070 Wuerzburg, Germany

Andrea Schwab

- University Hospital Wuerzburg, Department Tissue Engineering and Regenerative Medicine
- Present address: AO Research Institute Davos, Clavadelerstrasse 8, 7270 Davos, Switzerland
  E-Mail: andrea.schwab@aofoundation.org

Alexa Buss

- University Hospital Wuerzburg, Department Tissue Engineering and Regenerative Medicine, Roentgenring 11, 97070 Wuerzburg, Germany
- Present address: Klinikum Würzburg Mitte gGmbH, Juliusspital, Juliuspromenade 19, 97070 Wuerzburg, Germany
  E-Mail: alexa.buss@kwm-klinikum.de

Oliver Pullig

- University Hospital Wuerzburg, Department Tissue Engineering and Regenerative Medicine, Roentgenring 11, 97070 Wuerzburg, Germany
- Fraunhofer Institute for Silicate Research ISC, Translational Center Regenerative Therapies, Roentgenring 11, 97070 Wuerzburg, Germany

25 E-Mail: oliver.pullig@isc.fraunhofer.de

26 Franziska Ehlicke ([$]corresponding author)

27 • University Hospital Wuerzburg, Department Tissue Engineering and Regenerative Medicine,

28 Roentgenring 11, 97070 Wuerzburg, Germany

29 E-Mail: franziska.ehlicke@uni-wuerzburg.de

30 Phone: +49 931 3181900

31

32 Running title:

33 Cell-based chondral regeneration *ex vivo*

34

Abstract

Objective

Cartilage defect treatment strategies are dependent on the lesion size and severity. Osteochondral explants models are a platform to test cartilage repair strategies *ex vivo*. Current models lack in mimicking the variety of clinically relevant defect scenarios. In this controlled laboratory study, an automated device (artificial tissue cutter, ARTcut®) was implemented to reproducible create cartilage defects with controlled depth. In a pilot study, the effect of cartilage defect depth and oxygen tension on cartilage repair was investigated.

Design

Osteochondral explants were isolated from porcine condyles. 4 mm chondral and full thickness defects were treated with either porcine chondrocytes (CHON) or co-culture of 20 % CHON and 80 % MSC (MIX) embedded in collagen hydrogel. Explants were cultured with tissue specific media (without TGF-β) under normoxia (20 % O_2) and physiological hypoxia (2 % O_2). After 28 days, immune-histological stainings (Collagen II and X, Aggrecan) were scored (modified Bern-score, 3 independent scorer) to quantitatively compare treatments outcome.

Results

ARTcut® represents a software-controlled device for creation of uniform cartilage defects. Comparing the scoring results of the MIX and the CHON treatment, a positive relation between oxygen tension and defect depth was observed. Low oxygen tension stimulated cartilaginous matrix deposition in MIX group in chondral defects and CHON treatment in full thickness defects.

Conclusion

ARTcut® has proved a powerful tool to create cartilage defects and thus opens a wide range of novel applications of the osteochondral model, including the relation between oxygen tension and defect depth on cartilage repair.

Keywords

cartilage defect, *ex vivo* model, cartilage test system, chondrocytes, MSC, collagen type I hydrogel

1 Introduction

Defects of the articulating surface are frequently occuring diseases in the field of orthopedics, traumatology and sports medicine [1]. Around 14 % of patients who suffered from a trauma induced knee injury during their middle ages, including fractures of the tibia, fibula, femur, or patella, develop osteoarthritis in the same knee joint at later age (>65 years) [2]. High risk of failure of more than 20 % in cartilage defect repair require to rethink and improve current cartilage treatment concepts with the aim for long-term repair of cartilage defects [3, 4].

Due to the avascular and aneural character of adult articular cartilage, large defects do not heal spontaneously [5]. Defects that are classified according to International Cartilage Repair Society (ICRS) grade III (defect depth >50 % cartilage depth) and IV (defect reaches subchondral bone) need surgical intervention to repair [6]. Gold standard for defects larger than 2-3 cm^2 is the autologous chondrocyte implantation (ACI), resulting in similar outcome as microfracture [7, 8]. In a recent data analysis for cartilage defects, matrix-associated chondrocyte implantation (M-ACI) showed a significant lower reoperation rate than microfracture 2 years post-op [9]. M-ACI as well as ACI require two surgical interventions; the first to take a cartilage tissue sample for subsequent chondrocyte isolation and the second one for injection of isolated *in vitro* expanded autologous chondrocytes into defect site.

However, (M-)ACI has two main limitations: Due to the limited number of healthy and non-degenerated chondrocytes, cells have to be expanded *in vitro* to achieve sufficient number of cells needed for the implantation (ACI: 1 million cells per cm^2, M-ACI: 20 million cells per cm^3) [10-12]. Further, chondrocyte-based cartilage treatments, as well as microfracture techniques, result in formation of fibrocartilage,

83 characterized by its inferior mechanical properties and thus lacking functional restoration compared to
84 healthy hyaline cartilage [4, 13-17]. One approach to overcome the limitation of cell number for (M-)ACI
85 treatment are MSC-chondrocyte co-cultures, *e.g.*, 80 % MSC and 20 % chondrocytes, that reduces
86 autologous chondrocyte cell number at same total cell density. Co-cultures of MSCs and chondrocytes
87 have shown to increase cartilaginous matrix production and reduce hypertrophy, associated with MSCs
88 during chondrogenic differentiation [18, 19].
89 To bring cartilage treatments to the next level, cartilage repair needs to be studied and understood in
90 more detail, starting with basic research questions in a physiologically relevant environment.
91 An *ex vivo* cartilage defect test system based on osteochondral explants was established by Schwab *et al.*
92 [20]. This test system represents a valuable *ex vivo* platform for biomaterial evaluation in critical size
93 trauma-induced cartilage defects in terms of biocompatibility, biomaterial tissue integration and cartilage
94 repair with higher throughput compared to *in vivo* models. Separated media compartments of the culture
95 device allow for controlled, tissue- and cell-specific nutrient supply during *ex vivo* culture of osteochondral
96 explants. This model also allows direct comparison of different treatment approaches under controlled
97 conditions and has been shown to stimulate cartilage-like tissue formation of chondrocytes or MSCs in
98 osteochondral lesions [21, 22].
99 However, this defect model was limited to full thickness defects created with a biopsy punch. To date, the
100 creation of defects that do not fully penetrate the cartilage with the help of a biopsy punch or scalpel
101 suffer from low reproducibility and are dependent on the operator. Therefore, an automated device with
102 control over drilling depth to create defects with high reproducibility can overcome this limitation to study
103 chondral wound healing. Of note, the drilling should not harm surrounding cartilage tissue and cell
104 viability, neither by mechanical tissue disruption nor by friction induced heating. For the creation of
105 defects in hard tissues like cartilage or even bone, there is no device available for automated defect
106 creation that meets the above-mentioned requirements.

107 Following, in the present study the defect creation of the *ex vivo* defect model introduced by Schwab *et*
108 *al*. was modified by implementation of a semi-automated drilling device, originally developed to
109 mechanically induce standardized and reproducible wounds in full thickness skin equivalents [23]. Key
110 features of this artificial tissue cutter (ARTcut®) are the sensor controlled optical barrier in combination
111 with a moveable milling machine along x-, y- and z-axis. The light-barrier controlled drilling allows for
112 creation of defects with defined depths in a reproducible set-up. Creation of tissue defects with ARTcut®
113 can be performed under sterile conditions for subsequent *in vitro* or *ex vivo* culture with the possibility to
114 adjust defect geometry and control of defect creation process.
115 Another fact that has been neglected in the studies by Schwab *et al.* is the low oxygen tension present in
116 the articular capsule [24]. It has been shown in literature that low oxygen tension is an important stimulus
117 in chondrogenesis and increases the chondrogenic potential of articular cartilage progenitor cells and
118 MSCs [24-26]. Taken together, the present study aimed to implement the ARTcut® as tool for automated
119 wounding to the *ex vivo* model allowing to study the influence of defect depth (full thickness defects and
120 chondral defects) on tissue repair. In a pilot study, the relation between oxygen tension (normoxia 20 %
121 vs. physiological hypoxia 2 %), defect depth and treatment strategy was studied. For the treatment
122 strategies either chondrocytes only (CHON) or a mixture of 80 % MSC and 20 % CHON (MIX) were
123 embedded in a collagen type I hydrogel for implantation into cartilage defects in the *ex vivo* osteochondral
124 model without further supplementation of growth factors to elusively study the effect of the culture
125 conditions on cartilage repair.

126 2 Methods

127 2.1 Osteochondral cylinders: Isolation, defect creation and *ex vivo* culture

128 Osteochondral cylinders (diameter: 8 mm, height: 5 mm) were isolated from medial femoral condyles of
129 6-8-month-old domestic pigs as previously described [20]. Creation of defects in osteochondral cylinders

130 was carried out either manually or automatically, depending on the intended defect depth: Full thickness
131 defects were manually created with a biopsy punch (diameter 4 mm; Kai Medical, BPP-40F). Chondral
132 defects of 1 mm depth were created using custom-built ARTcut® (Figure 1A), a software-controlled device
133 for automatic wound placement in tissues developed by Fraunhofer ISC and IGB, Wuerzburg [23].
134 Osteochondral cylinders were fixed in support plate (Figure 1C) at specific x- and y-positions, and onset of
135 drilling 1 mm chondral defects (z-axis) was determined with light beam (Figure 1B). For more details on
136 the standardized defect creation process using ARTcut®, see chapter 1.2 in the supplementary
137 information.
138 After creation of full thickness or 1 mm chondral defects, the cartilage defects were filled with cell
139 embedded collagen type I hydrogels (Figure 2). For subsequent *ex vivo* culture, osteochondral explants
140 were transferred into custom-made culture platform [20] and cultured for 28 days with tissue specific
141 media (Table 1) changed every 3-4 days. The *ex vivo* culture was carried out in a humidified atmosphere
142 at 37°C and 5 % CO_2 (BBD 6220 CO_2 Incubator, Thermo Scientific™) either under normoxic (20 %) or
143 physiological hypoxic (2 %) conditions.

144 2.2 Chondrocyte and mesenchymal stromal cells (MSC): isolation and *in vitro* expansion

145 Porcine chondrocytes were isolated from lateral condyles of 6–8-month-old domestic pigs by enzymatic
146 digestion as previously described [20]. Chondrocytes were used at passage 0 – directly after isolation - for
147 embedding in collagen type I hydrogel.
148 Porcine MSC were isolated from bone marrow aspirate (iliac crest) under the approval (reference number:
149 55.2 2532-2-256) of the District Government of Lower Franconia and the local animal welfare committee
150 and performed according to the German Animal Welfare Act and the EU Directive 2010/63/EU according
151 to the procedure described in chapter 1.2 in the supplementary I.

152 ## 2.3 Cell embedding in collagen type I hydrogel

153 In a pilot study, cartilage defects were treated with collagen type I hydrogel (see chapter 1.3 in the
154 supplementary for details). For implantation, two different cell laden constructs, as illustrated in Figure 2,
155 were prepared and each cultured under normoxic and physiological hypoxic conditions. 1) CHON were
156 prepared by embedding of chondrocytes in collagen type I hydrogel without expansion at a final density
157 of 20 million cells/mL hydrogel volume; 2) MIX were prepared by mixing 80 % MSC with 20 % chondrocytes
158 at same cell density. CHON and MIX implants were filled into the cartilage defect for gelation at 37°C.

159 ## 2.4 Live-dead viability staining

160 To visualize a possible effect of defect creation process on cell viability of tissue samples, live-dead viability
161 staining was performed (live-dead staining kit for mammalian cells, L3224, Invitrogen). Osteochondral
162 explants were incubated with 4 µM Calcein AM and 2 µM ethidium homodimer-1 in DMEM HG and
163 visualized with fluorescence microscope (494 nm/517 nm and 517 nm/617 nm wavelength) Keyence BZ-
164 9000 (Biorevo). Living cells are stained by Calcein AM in green, dead cells are stained by ethidium
165 homodimer-1 in red.

166 ## 2.5 Histological evaluation

167 Osteochondral explants, harvested on day 0 and day 28, were washed with phosphate buffered saline,
168 fixed for 24 h with 4 % formalin (Roti Histofix, Carl Roth P087.3) and processed with plastic embedding
169 (Technovit T9100, Heraeus Kulzer, 66006735) as detailed described in the supplementary.

170 For immune-histological stainings, antigens were enzymatically retrieved depending on antibody (Table 2).
171 Before incubation with primary antibody over night at 4°C, slides were blocked with 3 % (v/v) H_2O_2 (Carl
172 Roth, 8070) and incubated with 5 % (w/v) bovine serum albumin. All stainings were visualized with
173 Horseradish-peroxidase kit (DCS Innovative, Dako, K3468) following manufacturer`s instructions. Cell
174 nuclei were counterstained with Mayer's hematoxylin (Morphisto, 11895), rehydrated and mounted with

175 Entellan (Merck, 1079610500). All washing steps between blocking or chemical incubation were
176 performed with PBS supplemented with 0.5 % Tween-20 (VWR, 8.22184).

177 2.6 Histological scoring

178 Histological scoring for the evaluation of the immune histological stainings (collagen II, X and aggrecan)
179 was performed. For in vitro tissue engineered samples the Bern score has been introduced, while cartilage
180 tissue repair in clinical studies can be evaluated based on the international cartilage repair society (ICRS)
181 score II [27]. Further, Chang et al. introduced a modified International cartilage repair society score by
182 adding two new criteria, namely the visual assessment of collagen type I and II staining [28]. The inclusion
183 of extracellular markers is an important step to better evaluate the composition of the repair matrix.
184 Therefore, in this pilot study, the scoring category A (Bern-score), originally evaluating the uniformity and
185 darkness of Safranin O-fast green stain, was translated to immune histological stainings of collagen type I,
186 II, X and aggrecan) [29]. Stained sections (*n*=2 biological replicates) were evaluated blinded by three
187 independent operators according to the criteria summarized in Table 3. Maximum possible score for the
188 here reported study was 12 points.

189 2.7 Statistics

190 Statistical analysis was performed with GraphPad Prism 6.07. Scoring values obtained from two
191 independent experiments, each evaluated by three examinators were used for statistical analysis,
192 resulting in $n = 6$ for each experimental group (Figure 2). Two groups differing in only one culture
193 parameter (oxygen tension, defect depth and applied cell type) were directly compared. Following tests
194 for outlier and Gaussian distribution, the data was either compared using an unpaired t-test (normally
195 distributed values) or a Mann-Whitney test (not normally distributed values). A p-value <0.05 was
196 considered statistically significant.

3 Results

3.1 Chondral defect creation with ARTcut®

ARTcut® (Figure 1) represents an automated device for reproducible creation of chondral defects (1 mm in depth; Figure 3A). Main advantage of using the ARTcut® is the ability to create defined chondral defects with a flat bottom to allow a tide and uniform contact with any solid pre-formed cylindrical implant, for example bioprinted constructs with flat bottom.

The laser beam to detect the surface of every single osteochondral explant is the unique feature of the ARTcut® to define the onset of the drilling, thus all defects result with the same depth. Chondral cartilage defect induced with ARTcut® appeared as a well-defined rectangular defect boundary in cross section (diameter: 4 mm, height: 1 mm) with flat bottom (Figure 3B). In contrast, the manually created defect (using biopsy punch) resulted in a half-round shape and required removing of residual cartilage tissue with a second tool (*e.g.,* a sharp spoon) shown in Figure 3C. Following, the accuracy of chondral defect geometry was much lower in manual procedure - using biopsy punch - compared to software – using automated ARTcut®.

The automated defect creation took less than 5 sec and thus heating of tissue due to friction and rotation during drilling was very unlikely. Microscopic images of live-dead stainings of osteochondral explants with 1 mm cartilage defects (diameter: 4 mm) confirmed no indications of cell death after tissue defect creation, neither with ARTcut® nor with biopsy punch (Figure 3D-E).

For the creation of full thickness cartilage defects, the ARTcut® was not required, since the bottom of the defect was given by the cartilage-bone interface. This two-tissue interface was easily separated using biopsy punch by pulling out the upper cartilage part.

3.2 Evaluation of cartilage treatments in the *ex vivo* model

Macroscopic images of all treatment and culture groups of the osteochondral *ex vivo* model after 28 days of culture are illustrated in Figure 4 A and B. The results of the pilot study demonstrated the feasibility and

221 reproducibility of the *ex vivo* cartilage test system as a platform to compare cartilage repair strategies.
222 Results of the adapted Bern scoring are shown in Figure 4 and Table 4 with scoring results of the co-culture
223 (MIX) being close to the CHON treatment in chondral and full thickness defects. Representative sections
224 of the scored samples are illustrated in Figure 5 and 6.

225 Under physiological hypoxic conditions, scoring results of defect repair after co-culture treatment (MIX)
226 was higher ($p = 0.0218$) in chondral defect than in full thickness defects. Scoring values of CHON treatment
227 in chondral and full thickness experimental groups did not differ much (n.s. $p = 0.1828$). At physiological
228 hypoxic conditions the scoring value was higher for CHON treatment compared to MIX treatment in full
229 thickness defects ($p = 0.0384$).

230 Under normoxic conditions, full thickness defects reached higher scoring values compared to the chondral
231 defects.

232 Comparing the outcome of same defect depth and treatment group (cell type), but cultured under
233 physiological hypoxic or normoxic conditions, the oxygen tension plays only a significant role in chondral
234 defects using MIX ($p = 0.0451$, higher scoring values under physiological hypoxic conditions) and in full
235 thickness defects treated with CHON ($p = 0.0316$, lower scoring values under physiological hypoxic
236 conditions).

237 Overall, treatment of the two defect depths with MIX showed slightly reduced scoring values compared
238 to the CHON treatment group. Only exception is MIX chondral (physiological hypoxia) with a slightly higher
239 value as the corresponding one for CHON. The results of the MIX treatment groups also tend to spread
240 more than the CHON treatment group independently of defect depth and oxygen tension.

241 4 Discussion

242 The choice of optimal treatment approach for cartilage repair is dependent on the size and depth of the
243 cartilage defect and thus the severity of pathological condition.

244 To mimic these different pathological defect scenarios, the implementation of the ARTcut® allowed to
245 overcome the low reproducibility of manual induced chondral defects. So far, there is no other automated
246 defect creation device published that has comparable features, namely possibility to select different
247 drilling parameters within one run and the application of one device for a wide range of soft and hard
248 tissues or tissue equivalents, as it is demonstrated with the ARTcut®. The induction of defects in
249 osteochondral explants allows to compare different cell-based treatment approaches by implantation of
250 cell loaded materials into the defects or to study the effect of defect depth on repair in an *ex vivo* model.
251 The software-controlled drilling parameters allow for standardized and reproducible defect creation in
252 other soft and hard tissues including bone tissue as well. *In vitro* as well as *ex vivo* studies require sample
253 procession at high throughput rates under a negative microbial environment. ARTcut® device addresses
254 these demands, resulting in higher methodological accuracy and reproducibility, compared to manual
255 procedure using biopsy punch.
256 Current treatments of small or large cartilage defects mainly aim on pain and symptom relief rather than
257 on functional tissue repair [30]. From a scientific point of view, there is way for improvement of cartilage
258 defects, especially on long term results. Material-assisted as well as cell-based therapies, including (M-)
259 ACI, AMIC and microfracture, tend to result in formation of mechanical inferior fibrocartilage in long term
260 follow up [30-32]. Moreover, the treatment of large defects with autologous cells are limited due to the
261 high number of chondrocytes needed for the current techniques. Therefore, in this laboratory-controlled
262 study, an *ex vivo* osteochondral defect model was modified to screen cell-based approaches to treat
263 chondral and full thickness cartilage defects. Different cell types, namely chondrocytes and MSCs, were
264 embedded in collagen type I hydrogel (CHON or MIX) and implanted in trauma induced chondral and full
265 thickness defects. A tendency of a stimulative and beneficial effect of MIX treatment (20 % CHON and 80 %
266 MSCs) was observed regarding cartilaginous matrix formation with the main advantage to reduce the
267 overall number of CHON used for traditional ACI treatment. It has been demonstrated in previous studies

268 that the cells in cartilage and subchondral bone remained metabolic active up to 56 days of *ex vivo* culture
269 [20].
270 Promising results regarding cartilage matrix production were obtained in this pilot study comparing CHON
271 and MIX in chondral and full thickness defects. The most pronounced increase in proteoglycan content
272 normalized to DNA amount resulted for the MIX treatment in both conditions, chondral and full thickness
273 defect, cultured under physiological hypoxia (Supplementary Figure S1). The MIX treatment reduces the
274 amount of autologous cartilage tissue needed for chondrocyte isolation, since chondrocytes represented
275 only 20 % of the total cell number in our model. Several *in vitro* studies and *in silico* models have shown
276 that chondrocytes in co-culture with MSCs increase the chondrogenic differentiation potential [18, 19, 33,
277 34]. Scalzone *et al.* reported of an enhanced chondrocyte activity measured by proteoglycan and collagen
278 type II production after co-culture with MSC compared to chondrocyte monoculture both embedded in
279 chitosan based hydrogels [19].
280 One advantage of the co-culture approach – when clinically applied – would be the one-step procedure,
281 addressing the surgical intervention of the knee joint, for the treatment of the cartilage defect: The
282 reduced number of chondrocytes in the MIX treatment can be isolated intra-operatively without
283 expansion and thus reduced the risk of chondrocyte dedifferentiation [35]. Further, the required MSCs,
284 *e.g.,* can be harvested independently form the knee surgery from bone marrow aspirate in a minimal
285 invasive procedure with subsequent expansion prior to the cartilage repair procedure to ensure a
286 sufficient number of MSCs.
287 Considering the absence of TGF-β in the culture media, which is known to drive MSC chondrogenesis and
288 matrix production [36], the here reported cartilage repair solely derives from the stimulating effect of the
289 surrounding osteochondral tissue, cell-cell signaling of the cell laden implants and the culture conditions.
290 Therefore, the overall matrix deposition is rather low due to missing stimuli of exogenous growth factors
291 in the here described model. Results of a similar *ex vivo* model, based on horse and bovine osteochondral

292 explants, suggested that the presence of the osteochondral tissue in the explants increase cartilage-like
293 matrix deposition compared to free swelling conditions of cell seeded material only [21, 22].
294 Beside the cell source, the influence of oxygen tension (normoxia 20 % O_2, physiological hypoxia 2 % O_2)
295 was studied during the *ex vivo* culture on chondrogenic matrix deposition, resulting in different outcomes
296 between the treatment groups in chondral and full thickness defects. Based on the histological scoring,
297 the results of the pilot study showed that the oxygen tension seems to only plays a role in chondral defects
298 - marked by elevated matrix production. In contrast, full thickness defects showed different response in
299 cartilage-like matrix deposition related to the treatment approach: While higher scoring values were
300 reached with CHON treatment under normoxic conditions, the pMIX treatment did not show differences
301 comparing physiological hypoxic and normoxic conditions. Physiological hypoxic conditions resulted in an
302 increase in cartilaginous matrix deposition in chondral defects compared to full thickness defects
303 independently of the used cell type (CHON, MIX). Once the defect reaches the cartilage-bone interface,
304 the cells in the implant receive stimuli from the subchondral bone that seem to counteract with the
305 hypoxic induced stimuli in the here presented model. One explanation of the differential cell response to
306 oxygen tension in chondral and full thickness defects may originate from the variation in oxygen tension
307 present in the human body. Chondrocytes are exposed to lower oxygen tension in avascular cartilage (2-
308 5 %) [37], synovial fluid and the synovial capsule (6.5-9.0 %) [25, 38], with an increasing oxygen level in the
309 bone marrow of subchondral bone (>7 %) [26, 39] and a maximum of 12 % in arterial blood [40]. Once the
310 cartilage defect progresses to the exposure of the subchondral bone in patients, chondrocytes within the
311 defect are exposed to higher levels of oxygen present in the bone supplied by vascular invasion [41]. It has
312 been shown that low oxygen inhibits the degradation of hypoxia induced factors (HIF) [42]. HIFs are
313 described to be essential for maintaining CHON homeostasis and extracellular matrix synthesis and
314 activate the transcription of genes [43].
315 While the here presented results of the pilot study are consistent, traceable and in line with literature,
316 there are still limitation in the current experimental setup: Due to limitations in availability of human

317 healthy osteochondral tissue – absence of any osteoarthritic phenotype – the authors decided to use
318 porcine tissue instead, as introduced by Schwab *et al.* [20]. The performance of an extensive comparative
319 *ex vivo* study comprising three parameters – namely 1) defect depth (chondral vs. full thickness), 2)
320 different cell types for defect filling and treatment (100 % chondrocytes vs. 20 % chondrocytes and 80 %
321 MSCs), and 3) oxygen tension (physiological hypoxia vs. normoxia) requires tissue material in the required
322 quantity and of similar quality. Due to the well-known donor issues associated with donor variability of
323 human tissue and the already mentioned limited availability of healthy human osteochondral tissue, this
324 could not be achieved for human tissue [44, 45]. In contrast, the use of porcine tissue isolated from one
325 pig population (similar age; grown up under equal conditions) minimizes the donor variation and
326 represents a tissue source for healthy and non-degenerated tissues with higher reproducibility. To proof
327 the findings and the trend of the here presented study and to show clear differences between treatment
328 groups, this experimental set-up needs to be repeated with more biological replicates.
329 The results obtained in this pilot study indicate that the surrounding tissue of the osteochondral explants
330 plays a crucial role in the defect repair, addressing chondral or full thickness defects, and that the oxygen
331 tension additionally stimulates the outcome in a defect depth dependent way. However, the exact
332 mechanism controlling success or failure of a treatment approach are not fully understood and require
333 further research. Despite the advantage of the here reported model, the mimicry of the complex 3D
334 environment present in the knee joint with the additional ability to reproducibly create (trauma induced)
335 defects, this model has its potential in pre-screening several biomaterials or treatment approaches, but
336 best candidates still require further pre-clinical and clinical testing to confirm obtained results.
337 To conclude, in this *ex vivo* study two cell-based approaches (CHON vs. MIX embedded in collagen type I
338 hydrogel) for the treatment of chondral and full thickness defects, cultured under normoxic and
339 physiological hypoxic conditions, were compared on their cartilage repair potential. Independently of
340 defect depth, the scoring results of the co-culture of chondrocytes and MSC (MIX) are close to those of
341 CHON treatment. Hence, usage of MIX could be a promising approach to reduce the number of

chondrocytes to one fifth and thus the amount of tissue for harvest and accompanied side morbidities for the patient. Further, in this experimental set up the oxygen tension showed an influence in a defect depth dependent way that has not been reported in literature before. The here presented advanced osteochondral cartilage defect model provides a promising platform to deeper understand the underlying mechanism.

Acknowledgements

The authors thank Andreas Diegeler (Fraunhofer ISC, Bronnbach) for technical support of the ARTcut®. Thanks also to Sebastian Naczenski for establishing the protocol for wounding of osteochondral explants using ARTcut® device. Finally, we would like to thank Heike Walles for her support. We acknowledge the authors of the thesis (Andrea Schwab and Alexa Buss) for the permission to use the data in this manuscript. Parts of the illustrations were produced in the light of a doctoral thesis (figure 1 and 3, with approval from Schwab 2017, German copyright law) [46] and a doctoral thesis (figure 5 and 6, with approval from Buss 2021) [47].

Author contribution

Conception and design of the study: Franziska Ehlicke and Andrea Schwab; Acquisition of data: Alexa Buss and Andrea Schwab; Analysis and interpretation of data: Andrea Schwab, Alexa Buss, Franziska Ehlicke and Oliver Pullig; Manuscript drafting: Andrea Schwab and Alexa Buss; Revision of the manuscript: Franziska Ehlicke and Oliver Pullig; Final approval: Franziska Ehlicke, Andrea Schwab, Alexa Buss and Oliver Pullig; Funding: Franziska Ehlicke and Alexa Buss.

Role of funding Sources

364 This work was financially supported by the European Union Seventh Framework Programme (FP7/2007-
365 2013) under grant agreement no 309962 (HydroZONES).A.Buss was supported by a medical scholarship of
366 the German Excellence Initiative to the Graduate School of Life Sciences, University of Würzburg. This
367 publication was supported by the Open Access Publication Fund of the University of Wuerzburg.

368 Conflict of interest statement

369 The authors declare no conflict of interest.

370 Ethics approval and consent to participate

371 Animal experiment was approved (reference number: 55.2 2532-2-256) by the District Government of
372 Lower Franconia and the local animal welfare committee and performed according to the German Animal
373 Welfare Act and the EU Directive 2010/63/EU. Following heparinization of the pig, porcine MSCs were
374 obtained by bone marrow aspiration.

375 # References

376 [1] W. Widuchowski, J. Widuchowski, T. Trzaska, Articular cartilage defects: study of 25,124
377 knee arthroscopies, Knee 14(3) (2007) 177-82. https://doi.org/10.1016/j.knee.2007.02.001.
378 [2] A.C. Gelber, M.C. Hochberg, L.A. Mead, N.Y. Wang, F.M. Wigley, M.J. Klag, Joint injury in
379 young adults and risk for subsequent knee and hip osteoarthritis, Ann Intern Med 133(5) (2000)
380 321-8. https://doi.org/10.7326/0003-4819-133-5-200009050-00007.
381 [3] A.R. Martín, J.M. Patel, H.M. Zlotnick, J.L. Carey, R.L. Mauck, Emerging therapies for cartilage
382 regeneration in currently excluded 'red knee' populations, npj Regenerative Medicine 4(1)
383 (2019) 12. https://doi.org/10.1038/s41536-019-0074-7.
384 [4] J.D. Wylie, M.K. Hartley, A.L. Kapron, S.K. Aoki, T.G. Maak, Failures and Reoperations After
385 Matrix-Assisted Cartilage Repair of the Knee: A Systematic Review, Arthroscopy 32(2) (2016)
386 386-92. https://doi.org/10.1016/j.arthro.2015.07.025.
387 [5] A.J. Sophia Fox, A. Bedi, S.A. Rodeo, The basic science of articular cartilage: structure,
388 composition, and function, Sports Health 1(6) (2009) 461-8.
389 https://doi.org/10.1177/1941738109350438.
390 [6] E.A. Makris, A.H. Gomoll, K.N. Malizos, J.C. Hu, K.A. Athanasiou, Repair and tissue
391 engineering techniques for articular cartilage, Nat Rev Rheumatol 11(1) (2015) 21-34.
392 https://doi.org/10.1038/nrrheum.2014.157.
393 [7] B.J. Cole, C. Pascual-Garrido, R.C. Grumet, Surgical management of articular cartilage defects
394 in the knee, J Bone Joint Surg Am 91(7) (2009) 1778-90.
395 [8] A.K. Dewan, M.A. Gibson, J.H. Elisseeff, M.E. Trice, Evolution of autologous chondrocyte
396 repair and comparison to other cartilage repair techniques, Biomed Res Int 2014 (2014) 272481.
397 https://doi.org/10.1155/2014/272481.
398 [9] P. Niemeyer, T. Schubert, M. Grebe, A. Hoburg, Matrix-Associated Chondrocyte Implantation
399 Is Associated With Fewer Reoperations Than Microfracture: Results of a Population-
400 Representative, Matched-Pair Claims Data Analysis for Cartilage Defects of the Knee, Orthop J
401 Sports Med 7(10) (2019) 2325967119877847. https://doi.org/10.1177/2325967119877847.
402 [10] M. Brittberg, A. Lindahl, A. Nilsson, C. Ohlsson, O. Isaksson, L. Peterson, Treatment of deep
403 cartilage defects in the knee with autologous chondrocyte transplantation, N Engl J Med 331(14)
404 (1994) 889-95. https://doi.org/10.1056/NEJM199410063311401.
405 [11] M. Mumme, A. Barbero, S. Miot, A. Wixmerten, S. Feliciano, F. Wolf, A.M. Asnaghi, D.
406 Baumhoer, O. Bieri, M. Kretzschmar, G. Pagenstert, M. Haug, D.J. Schaefer, I. Martin, M. Jakob,
407 Nasal chondrocyte-based engineered autologous cartilage tissue for repair of articular cartilage
408 defects: an observational first-in-human trial, Lancet (London, England) 388(10055) (2016)
409 1985-1994. https://doi.org/10.1016/S0140-6736(16)31658-0.
410 [12] R.L. Davies, N.J. Kuiper, Regenerative Medicine: A Review of the Evolution of Autologous
411 Chondrocyte Implantation (ACI) Therapy, Bioengineering (Basel) 6(1) (2019)
412 https://doi.org/10.3390/bioengineering6010022.
413 [13] J.D. Lamplot, K.A. Schafer, M.J. Matava, Treatment of Failed Articular Cartilage
414 Reconstructive Procedures of the Knee: A Systematic Review, Orthop J Sports Med 6(3) (2018)
415 2325967118761871. https://doi.org/10.1177/2325967118761871.

416 [14] G. Merkely, T. Ogura, J. Ackermann, A. Barbieri Mestriner, A.H. Gomoll, Clinical Outcomes
417 after Revision of Autologous Chondrocyte Implantation to Osteochondral Allograft
418 Transplantation for Large Chondral Defects: A Comparative Matched-Group Analysis, Cartilage
419 (2019) 1947603519833136. https://doi.org/10.1177/1947603519833136.
420 [15] K. Mithoefer, T. McAdams, R.J. Williams, P.C. Kreuz, B.R. Mandelbaum, Clinical efficacy of
421 the microfracture technique for articular cartilage repair in the knee: an evidence-based
422 systematic analysis, Am J Sports Med 37(10) (2009) 2053-63.
423 https://doi.org/10.1177/0363546508328414.
424 [16] P.C. Kreuz, M.R. Steinwachs, C. Erggelet, S.J. Krause, G. Konrad, M. Uhl, N. Sudkamp, Results
425 after microfracture of full-thickness chondral defects in different compartments in the knee,
426 Osteoarthritis Cartilage 14(11) (2006) 1119-25. https://doi.org/10.1016/j.joca.2006.05.003.
427 [17] J.L. Carey, Fibrocartilage Following Microfracture Is Not as Robust as Native Articular
428 Cartilage: Commentary on an article by Aaron J. Krych, MD, et al.: "Activity Levels Are Higher
429 After Osteochondral Autograft Transfer Mosaicplasty Than After Microfracture for Articular
430 Cartilage Defects of the Knee. A Retrospective Comparative Study", JBJS 94(11) (2012).
431 [18] L. Bian, D.Y. Zhai, R.L. Mauck, J.A. Burdick, Coculture of human mesenchymal stem cells and
432 articular chondrocytes reduces hypertrophy and enhances functional properties of engineered
433 cartilage, Tissue engineering. Part A 17(7-8) (2011) 1137-1145.
434 https://doi.org/10.1089/ten.TEA.2010.0531.
435 [19] A. Scalzone, A.M. Ferreira, C. Tonda-Turo, G. Ciardelli, K. Dalgarno, P. Gentile, The interplay
436 between chondrocyte spheroids and mesenchymal stem cells boosts cartilage regeneration
437 within a 3D natural-based hydrogel, Sci Rep 9(1) (2019) 14630. https://doi.org/10.1038/s41598-
438 019-51070-7.
439 [20] A. Schwab, A. Meeuwsen, F. Ehlicke, J. Hansmann, L. Mulder, A. Smits, H. Walles, L. Kock, Ex
440 vivo culture platform for assessment of cartilage repair treatment strategies, ALTEX 34(2) (2017)
441 267-277. https://doi.org/10.14573/altex.1607111.
442 [21] V.H.M. Mouser, N.M.M. Dautzenberg, R. Levato, M.H.P. van Rijen, W.J.A. Dhert, J. Malda, D.
443 Gawlitta, Ex vivo model unravelling cell distribution effect in hydrogels for cartilage repair,
444 ALTEX 35(1) (2018) 65-76. https://doi.org/10.14573/altex.1704171.
445 [22] M.L. de Vries-van Melle, R. Narcisi, N. Kops, W.J. Koevoet, P.K. Bos, J.M. Murphy, J.A.
446 Verhaar, P.M. van der Kraan, G.J. van Osch, Chondrogenesis of mesenchymal stem cells in an
447 osteochondral environment is mediated by the subchondral bone, Tissue Eng Part A 20(1-2)
448 (2014) 23-33. https://doi.org/10.1089/ten.TEA.2013.0080.
449 [23] A. Rossi, A. Appelt-Menzel, S. Kurdyn, H. Walles, F. Groeber, Generation of a three-
450 dimensional full thickness skin equivalent and automated wounding, J Vis Exp (96) (2015)
451 https://doi.org/10.3791/52576.
452 [24] G. Pattappa, R. Schewior, I. Hofmeister, J. Seja, J. Zellner, B. Johnstone, D. Docheva, P.
453 Angele, Physioxia Has a Beneficial Effect on Cartilage Matrix Production in Interleukin-1 Beta-
454 Inhibited Mesenchymal Stem Cell Chondrogenesis, Cells 8(8) (2019)
455 https://doi.org/10.3390/cells8080936.
456 [25] G. Pattappa, B. Johnstone, J. Zellner, D. Docheva, P. Angele, The Importance of Physioxia in
457 Mesenchymal Stem Cell Chondrogenesis and the Mechanisms Controlling Its Response, Int J Mol
458 Sci 20(3) (2019) https://doi.org/10.3390/ijms20030484.

459 [26] D.E. Anderson, B.D. Markway, D. Bond, H.E. McCarthy, B. Johnstone, Responses to altered
460 oxygen tension are distinct between human stem cells of high and low chondrogenic capacity,
461 Stem Cell Res Ther 7(1) (2016) 154. https://doi.org/10.1186/s13287-016-0419-8.
462 [27] M. Rutgers, M.J.P. van Pelt, W.J.A. Dhert, L.B. Creemers, D.B.F. Saris, Evaluation of
463 histological scoring systems for tissue-engineered, repaired and osteoarthritic cartilage,
464 Osteoarthritis and Cartilage 18(1) (2010) 12-23.
465 https://doi.org/https://doi.org/10.1016/j.joca.2009.08.009.
466 [28] F. Chang, T. Ishii, T. Yanai, H. Mishima, H. Akaogi, T. Ogawa, N. Ochiai, Repair of large full-
467 thickness articular cartilage defects by transplantation of autologous uncultured bone-marrow-
468 derived mononuclear cells, Journal of Orthopaedic Research 26(1) (2008) 18-26.
469 https://doi.org/https://doi.org/10.1002/jor.20470.
470 [29] S.P. Grogan, A. Barbero, V. Winkelmann, F. Rieser, J.S. Fitzsimmons, S. O'Driscoll, I. Martin,
471 P. Mainil-Varlet, Visual Histological Grading System for the Evaluation of in Vitro–Generated
472 Neocartilage, Tissue Engineering 12(8) (2006) 2141-2149.
473 https://doi.org/10.1089/ten.2006.12.2141.
474 [30] U. Horas, D. Pelinkovic, G. Herr, T. Aigner, R. Schnettler, Autologous chondrocyte
475 implantation and osteochondral cylinder transplantation in cartilage repair of the knee joint. A
476 prospective, comparative trial, J Bone Joint Surg Am 85(2) (2003) 185-92.
477 https://doi.org/10.2106/00004623-200302000-00001.
478 [31] J.R. Steadman, K.K. Briggs, J.J. Rodrigo, M.S. Kocher, T.J. Gill, W.G. Rodkey, Outcomes of
479 microfracture for traumatic chondral defects of the knee: average 11-year follow-up,
480 Arthroscopy 19(5) (2003) 477-84. https://doi.org/10.1053/jars.2003.50112.
481 [32] J.L. Carey, Fibrocartilage following microfracture is not as robust as native articular
482 cartilage: commentary on an article by Aaron J. Krych, MD, et al.: "Activity levels are higher after
483 osteochondral autograft transfer mosaicplasty than after microfracture for articular cartilage
484 defects of the knee. A retrospective comparative study", J Bone Joint Surg Am 94(11) (2012)
485 e80. https://doi.org/10.2106/JBJS.L.00319.
486 [33] M.J. Chen, J.P. Whiteley, C.P. Please, A. Schwab, F. Ehlicke, S.L. Waters, H.M. Byrne,
487 Inducing chondrogenesis in MSC/chondrocyte co-cultures using exogenous TGF-β: a
488 mathematical model, Journal of Theoretical Biology 439 (2018) 1-13.
489 https://doi.org/https://doi.org/10.1016/j.jtbi.2017.11.024.
490 [34] T.W. Kim, M.C. Lee, H.C. Bae, H.-S. Han, Direct Coculture of Human Chondrocytes and
491 Synovium-Derived Stem Cells Enhances In Vitro Chondrogenesis, Cell J 20(1) (2018) 53-60.
492 https://doi.org/10.22074/cellj.2018.5025.
493 [35] K. von der Mark, V. Gauss, H. von der Mark, P. Muller, Relationship between cell shape and
494 type of collagen synthesised as chondrocytes lose their cartilage phenotype in culture, Nature
495 267(5611) (1977) 531-2. https://doi.org/10.1038/267531a0.
496 [36] B. Johnstone, T.M. Hering, A.I. Caplan, V.M. Goldberg, J.U. Yoo, In vitro chondrogenesis of
497 bone marrow-derived mesenchymal progenitor cells, Exp Cell Res 238(1) (1998) 265-72.
498 https://doi.org/10.1006/excr.1997.3858.
499 [37] S. Zhou, Z. Cui, J.P.G. Urban, Factors influencing the oxygen concentration gradient from
500 the synovial surface of articular cartilage to the cartilage–bone interface: A modeling study,
501 Arthritis & Rheumatism 50(12) (2004) 3915-3924. https://doi.org/10.1002/art.20675.

502 [38] K. Lund-Olesen, Oxygen tension in synovial fluids, Arthritis Rheum 13(6) (1970) 769-76.
503 https://doi.org/10.1002/art.1780130606.
504 [39] A. Carreau, B. El Hafny-Rahbi, A. Matejuk, C. Grillon, C. Kieda, Why is the partial oxygen
505 pressure of human tissues a crucial parameter? Small molecules and hypoxia, J Cell Mol Med
506 15(6) (2011) 1239-53. https://doi.org/10.1111/j.1582-4934.2011.01258.x.
507 [40] M. Marenzana, T.R. Arnett, The Key Role of the Blood Supply to Bone, Bone Research 1(1)
508 (2013) 203-215. https://doi.org/10.4248/BR201303001.
509 [41] J. Filipowska, K.A. Tomaszewski, L. Niedzwiedzki, J.A. Walocha, T. Niedzwiedzki, The role of
510 vasculature in bone development, regeneration and proper systemic functioning, Angiogenesis
511 20(3) (2017) 291-302. https://doi.org/10.1007/s10456-017-9541-1.
512 [42] A. Kremer, M. Wussmann, M. Herrmann, M. Raghunath, H. Walles, Ciclopirox olamine
513 promotes the angiogenic response of endothelial cells and mesenchymal stem cells, Clin
514 Hemorheol Microcirc 73(2) (2019) 317-328. https://doi.org/10.3233/CH-190559.
515 [43] J. Fernandez-Torres, Y. Zamudio-Cuevas, G.A. Martinez-Nava, A.G. Lopez-Reyes, Hypoxia-
516 Inducible Factors (HIFs) in the articular cartilage: a systematic review, Eur Rev Med Pharmacol
517 Sci 21(12) (2017) 2800-2810.
518 [44] H.X. Chang, L. Yang, Z. Li, G. Chen, G. Dai, Age-related biological characterization of
519 mesenchymal progenitor cells in human articular cartilage, Orthopedics 34(8) (2011) e382-8.
520 https://doi.org/10.3928/01477447-20110627-06.
521 [45] M. Kim, I.E. Erickson, A.H. Huang, S.T. Garrity, R.L. Mauck, D.R. Steinberg, Donor Variation
522 and Optimization of Human Mesenchymal Stem Cell Chondrogenesis in Hyaluronic Acid, Tissue
523 Eng Part A 24(21-22) (2018) 1693-1703. https://doi.org/10.1089/ten.TEA.2017.0520.
524 [46] A. Schwab, Development of an osteochondral cartilage defect model, Julius-Maximilians
525 University, Wuerzburg 2017.
526 [47] A. Buss, Evaluation of cartilage regeneration strategies in an osteochondral ex vivo cartilage
527 defect model, Julius-Maximilians University, Wuerzburg 2021.

528

Figure Legends

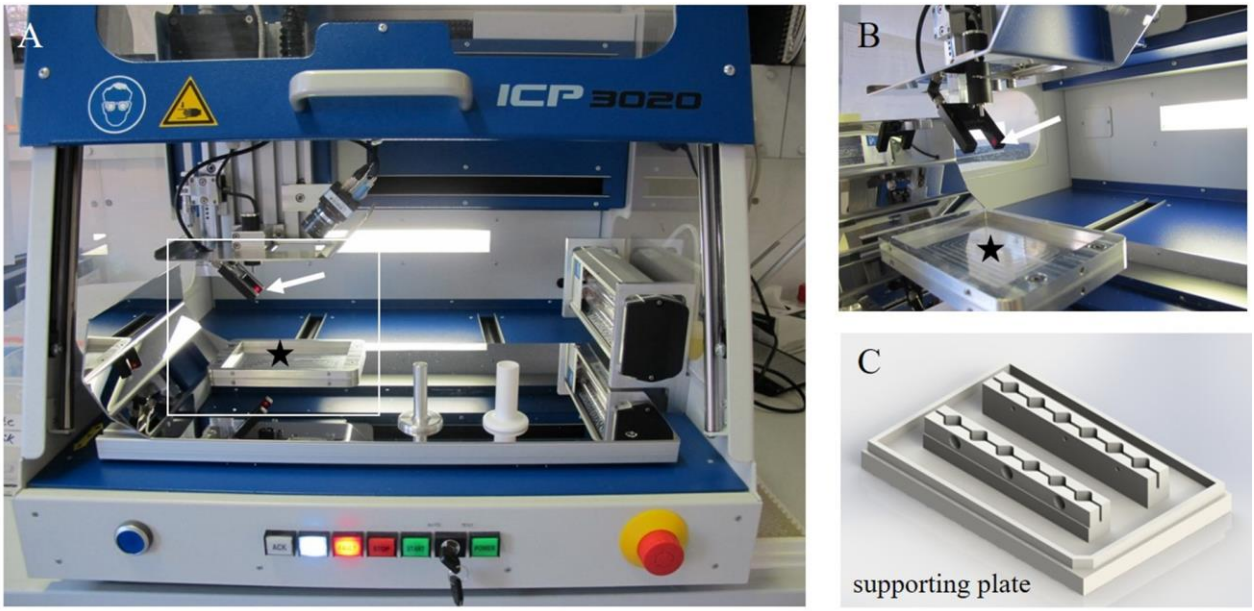

Figure 1: Artificial tissue cutter (ARTcut®): A) View of the computerized numerical controlled device equipped with B) optical barrier (white arrow indicates the laser light beam) and a C) supporting plate to fix the samples and place on the bottom of the machine (marked with black star).

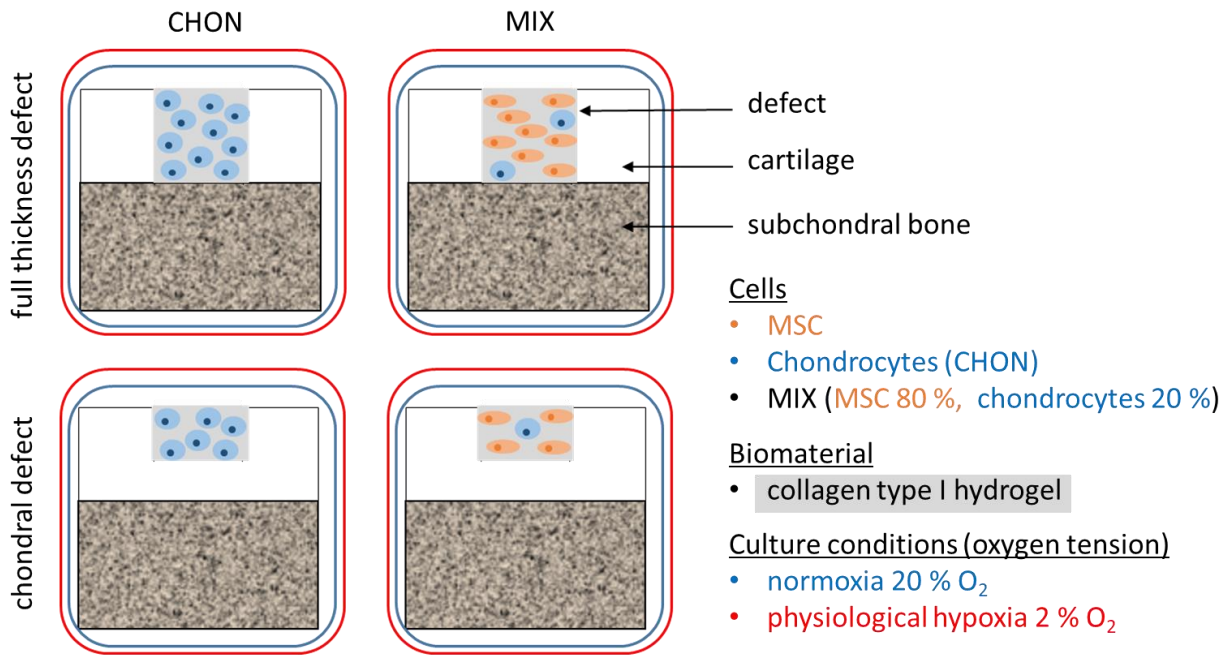

536

537 Figure 2: Schematic overview of all experimental groups: Full thickness and chondral defects of
538 osteochondral explants were treated with collagen type I hydrogel (grey) either containing chondrocytes
539 (CHON, blue) or MIX (80 % MSC [orange] and 20 % chondrocytes), implanted in chondral or full thickness
540 defects and cultured *ex vivo* under normoxic (20 % O_2, blue frame) or physiological hypoxic conditions (2 %
541 O_2, red frame).

542

543

544

545

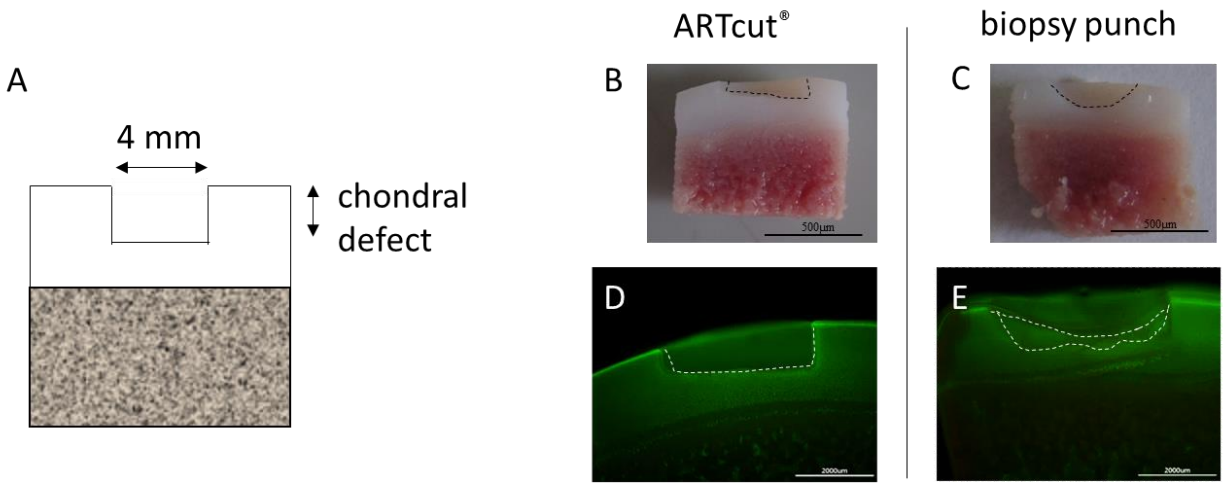

Figure 3: Osteochondral explant cross section with chondral defect. A) Schematic illustration of A) 4 mm chondral defect. B-E) Comparison of chondral defect created automated with ARTcut® (B) and manually with biopsy punch (C) (scale bar 500 µm). D-E) Live-dead staining of explant cross section highlighting accurate borders of defect induced with ARTcut® (D) and more irregular shaped geometry of manually induced defect (E) (scale bar 200 µm).

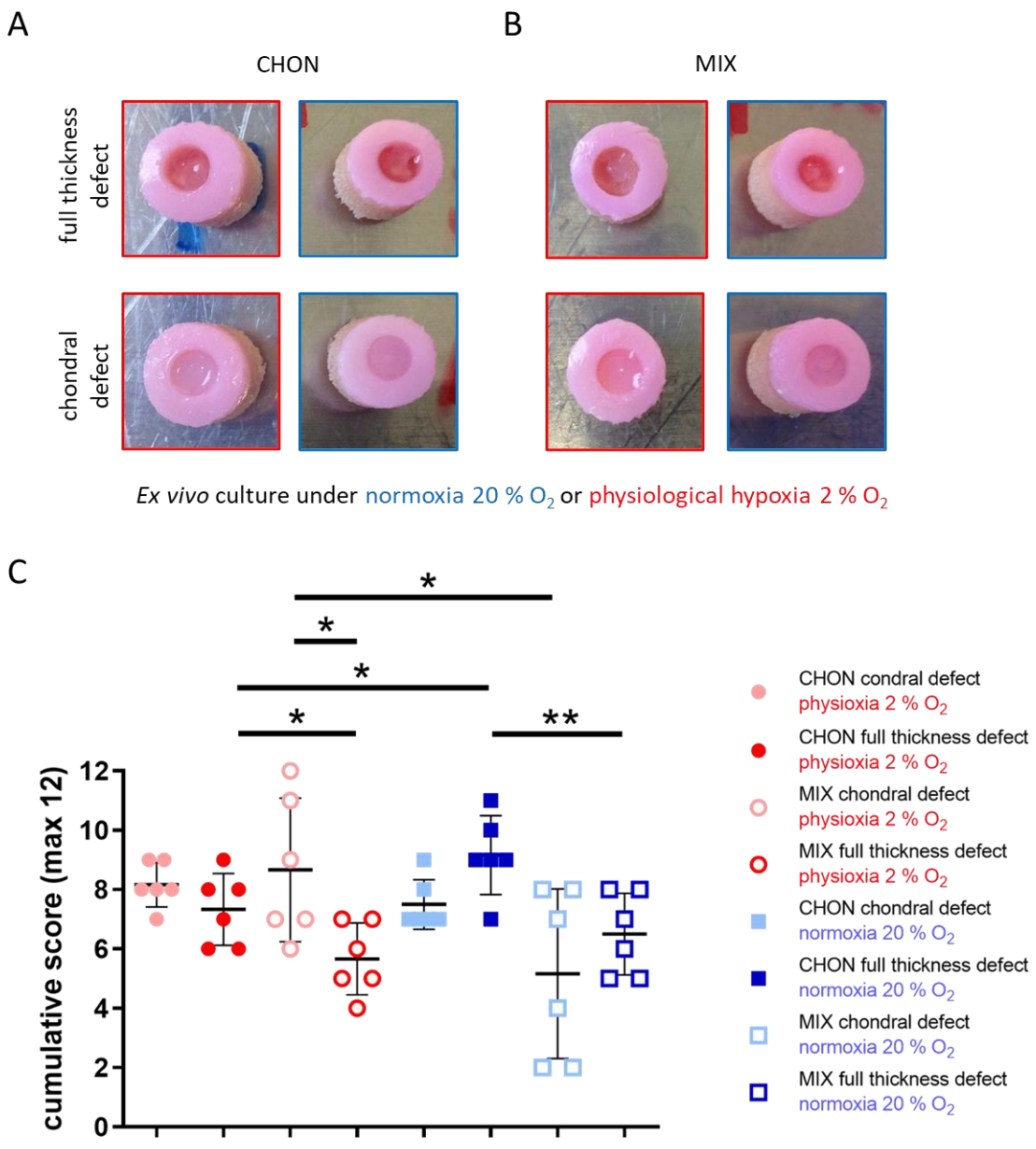

Figure 4: Evaluation of defect repair after 28 days *ex vivo* culture. Macroscopic images of full thickness and chondral defects (diameter 4 mm) treated with A) porcine chondrocytes (CHON) or B) co-culture of porcine MSC and CHON (MIX). Red frame indicates culture under physiological hypoxic, blue frame under normoxic oxygen tension. Macroscopically, there are no obvious differences comparing full thickness and chondral defects. C) Scoring evaluation of cartilage repair strategies in the *ex vivo* model (mean ± standard deviation with single scoring results as dots resp. listed values for 1st and 2nd biological replicate). Unpaired t-test or Mann-Whitney test * $p < 0.05$, ** $p < 0.01$.

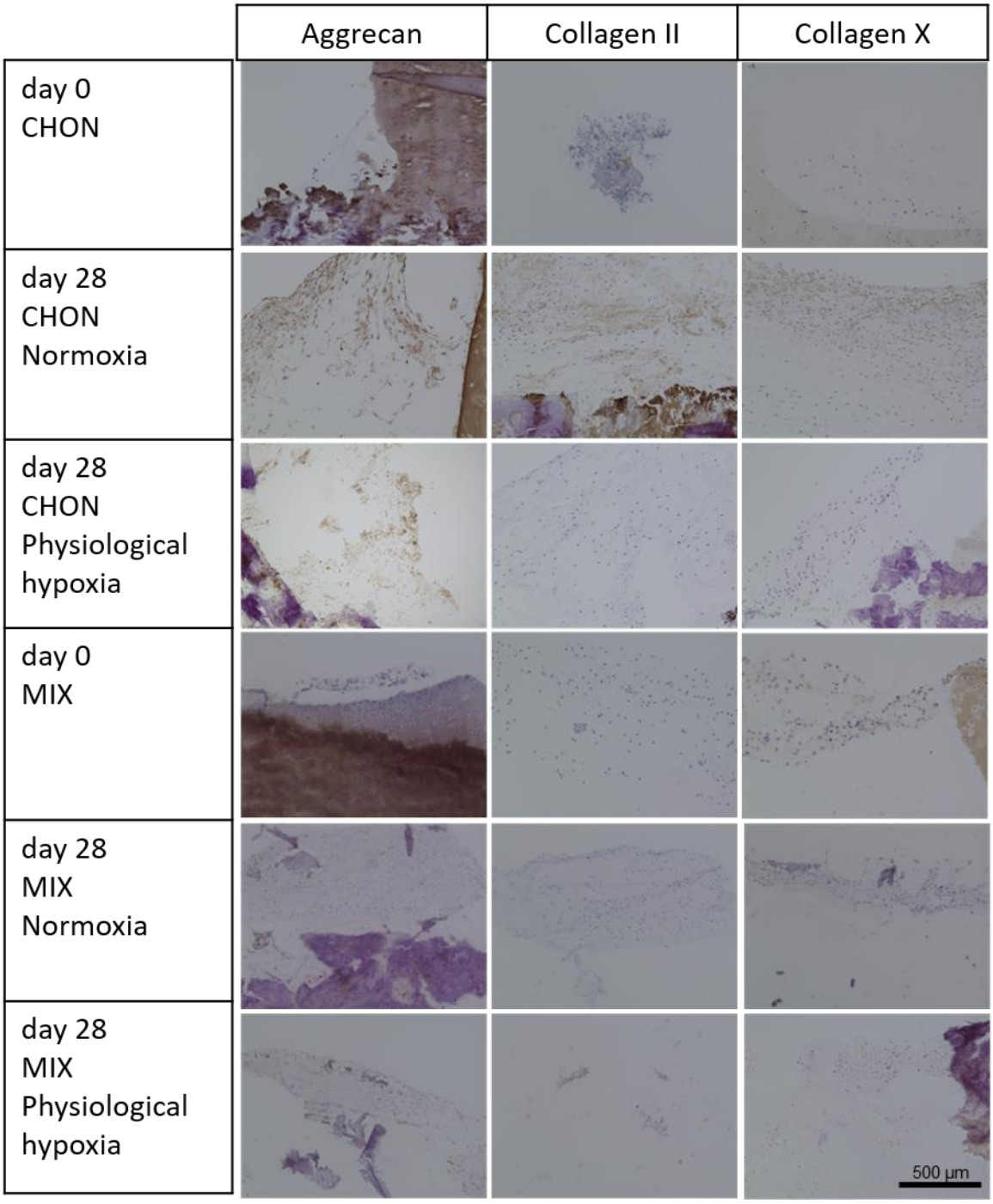

Figure 5: Chondral defects of the osteochondral defect model treated with either chondrocytes (CHON) or MSC-chondrocyte co-culture (MIX) embedded in a collagen hydrogel. Histological stainings of cross sections showing the defect area at day 0 and after 28 days of ex vivo culture under normoxic (20 % O_2) or physiological hypoxic (2 % O_2 conditions. Scale bar 500 µm.

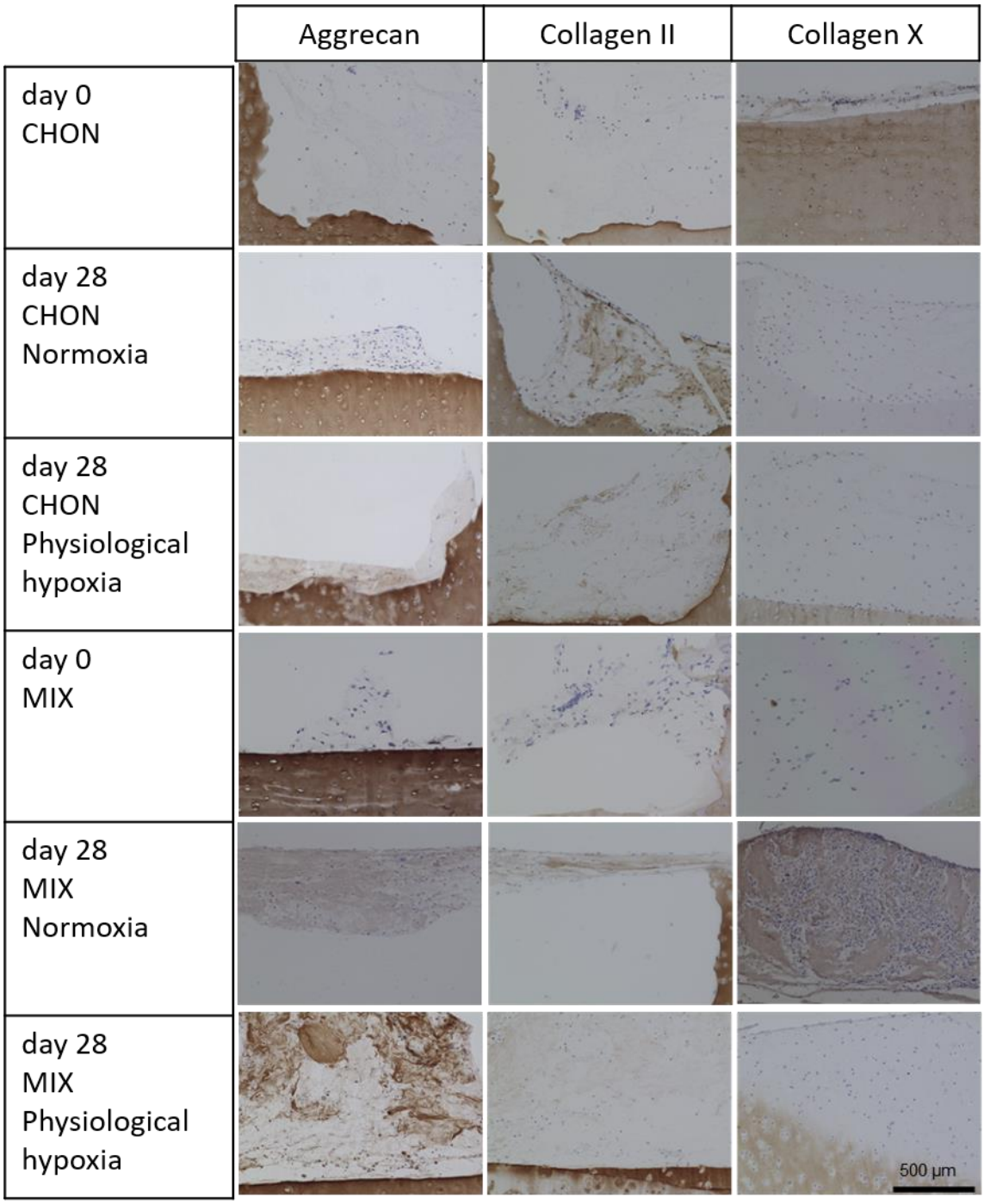

Figure 6: Full thickness cartilage defects of the osteochondral defect model treated with either chondrocytes (CHON) or MSC-chondrocyte co-culture (MIX) embedded in a collagen hydrogel. Histological stainings of cross sections showing the defect area at day 0 and after 28 days of ex vivo culture under normoxic (20 % O_2) or physiological hypoxic (2 % O_2) conditions. Scale bar 500 µm.

574 Table 1: Composition of bone and cartilage media for *ex vivo* culture of osteochondral explants.

	Cartilage media	Bone media	Supplier
DMEM GlutaMAX (high glucose)	98 %	89 %	Gibco 61965
Antibiotics	10 U/mL penicillin, 10 µg/mL Streptomycin, 0.25 µg/mL Amphotericin (1 % (v/v))	10 U/mL penicillin, 10 µg/mL Streptomycin, 0.25 µg/mL Amphotericin (1 % (v/v))	Gibco, 15240
Sodium-pyruvate	1 mM	-	Gibco, 11360
L-ascorbic acid-2-phosphate	50 µg/mL	50 µg/mL	Wako chemicals, 013-19641
L-proline	40 µg/mL	-	Sigma-Aldrich, P5607
Dexamethasone	100 nM	100 nM	Sigma-Aldrich, D4902
fetal bovine serum (FBS)		10 % (v/v)	Gibco, 10270106
Insulin-transferrin-selenin	1 % (v/v)	-	ITS^{+}-premix, Gibco, Life Technologies, 32430
β-glycerophosphate	-	10 mM	Sigma-Aldrich, G9422

575

576 Table 2: List of antibodies for immune-histological stainings.

Antibody	clone	Dilution and final antibody concentration	Antigen retrieval	Antibody supplier
Collagen type I	EPR7785	1:1000; 0.875 µg/mL	pepsin & hyaluronidase	Abcam, ab138492
Collagen type II	II-4C11	1:1000; 1 µg/mL	pepsin & hyaluronidase	MP Bio, 63171
Collagen type X	COL-10	1:4000; 0.25 µg/mL	pronase	Sigma-Aldrich, C7974
Aggrecan	EPR7785	1:2000; 0.5 µg/mL	pronase	Invitrogen, AHP0012

577

578 Table 3: Criteria for evaluating immune histological stainings with a maximum of 12 points (0-3 scores for each criteria assessing
579 the uniformity and darkness of aggrecan, collagen type I, II and X staining). Table adapted from Grogan et al. and Chang et al.
580 [28, 29].

Uniformity and darkness of aggrecan stain
0: No stain, 1: Weak staining of poorly formed matrix, 2: Moderately even staining, 3: Even dark stain
Uniformity and darkness of collagen type II stain
0: No stain, 1: Weak staining of poorly formed matrix, 2: Moderately even staining, 3: Even dark stain
Uniformity and darkness of collagen type I stain
3: No stain, 2: Weak staining of poorly formed matrix, 1: Moderately even staining, 0: Even dark stain
Uniformity and darkness of collagen type X stain
3: No stain, 2: Weak staining of poorly formed matrix, 1: Moderately even staining, 0: Even dark stain

581

582 Table 4: Scoring results to evaluate cartilage repair strategies in the ex vivo model. The table summarized the cumulative score
583 of the 3-independent scorer (mean ± standard deviation with single scoring results of both biological replicate) for the CHON
584 (100 % chondrocytes) and MIX (20 % chondrocytes, 80 % MSCs) treatment of the full thickness and chondral defects after 28
585 days culture. Values for samples cultured under physiological hypoxia (2 % O2) and normoxia (20 % O2) are displayed in
586 separate columns.

		CHON		**MIX**	
	Cumulative score (max 12)	**Physiological hypoxia (2 % O_2)**	**Normoxia (20 % O_2)**	**Physiological hypoxia (2 % O_2)**	**Normoxia (20 % O_2)**
full thickness defect	1st biological replicate	9; 8; 8	9; 9; 7	6; 7; 4	8; 8; 7
	2nd biological replicate	7; 6; 6	9; 11; 10	5; 7; 5	5; 5; 6
	Mean ± standard deviation	**7.33 ± 1.21**	**9.17 ± 1.33**	**5.67 ± 1.21**	**6.5 ± 1.38**
chondral defect	1st biological replicate	7; 8; 9	7; 7; 7	11; 9; 12	4; 2; 2
	2nd biological replicate	8; 9; 8	9; 8; 7	7; 7; 6	8; 8; 7
	Mean ± standard deviation	**8.17 ± 0.75**	**7.50 ± 0.84**	**8.67 ± 2.42**	**5.17 ± 2.86**

587